

Physicochemical Characterization of Nebulized Superparamagnetic Iron Oxide Nanoparticles (SPIONs)

Halshka Graczyk, MSPH,¹ Louise C. Bryan, BSc,² Nastassja Lewinski, PhD,¹ Guillaume Suarez, PhD,¹ Geraldine Coullerez, PhD,² Paul Bowen, PhD,² and Michael Riediker, PhD^{1,3}

Abstract

Background: Aerosol-mediated delivery of nano-based therapeutics to the lung has emerged as a promising alternative for treatment and prevention of lung diseases. Superparamagnetic iron oxide nanoparticles (SPIONs) have attracted significant attention for such applications due to their biocompatibility and magnetic properties. However, information is lacking about the characteristics of nebulized SPIONs for use as a therapeutic aerosol. To address this need, we conducted a physicochemical characterization of nebulized Rienso, a SPION-based formulation for intravenous treatment of anemia.

Methods: Four different concentrations of SPION suspensions were nebulized with a one-jet nebulizer. Particle size was measured in suspension by transmission electron microscopy (TEM), photon correlation spectroscopy (PCS), and nanoparticle tracking analysis (NTA), and in the aerosol by a scanning mobility particle sizer (SMPS).

Results: The average particle size in suspension as measured by TEM, PCS, and NTA was 9 ± 2 nm, 27 ± 7 nm, and 56 ± 10 nm, respectively. The particle size in suspension remained the same before and after the nebulization process. However, after aerosol collection in an impinger, the suspended particle size increased to 159 ± 46 nm as measured by NTA. The aerosol particle concentration increased linearly with increasing suspension concentration, and the aerodynamic diameter remained relatively stable at around 75 nm as measured by SMPS.

Conclusions: We demonstrated that the total number and particle size in the aerosol were modulated as a function of the initial concentration in the nebulizer. The data obtained mark the first known independent characterization of nebulized Rienso and, as such, provide critical information on the behavior of Rienso nanoparticles in an aerosol. The data obtained in this study add new knowledge to the existing body of literature on potential applications of SPION suspensions as inhaled aerosol therapeutics.

Key words: nebulizer, aerosol distribution, inhaled therapy, characterization, SPIONs, Rienso

Introduction

ENGINEERED NANOPARTICLES have gained increased attention for a number of biomedical and bioengineering applications. Namely, new applications of nanomaterials in the field of biomedicine have sparked significant interest as a route of therapeutic drug delivery to the lungs for both local and systemic treatments. The lungs represent an excellent entry portal for aerosolized nanoparticles due to their high surface area, thin epithelial barriers, and extensive vasculature.⁽¹⁾ Inhaled nanoparticles have been shown to deposit with high efficiency throughout the entire respiratory tract,

from the extrapulmonary airways to the intrapulmonary regions, and subsequently undergo numerous transport processes within pulmonary tissues.^(2,3) An advantage of aerosolized nanoparticle formulations for pulmonary drug delivery is the fact that they demonstrate enhanced dispersion properties, as particles with a diameter of $< 1 \mu\text{m}$ are more easily incorporated in the respirable percentage of aerosolized droplets. Furthermore, certain biocompatible nanoparticles offer the potential for enhanced intracellular drug delivery.⁽⁴⁾

Nevertheless, nanomedicine currently lacks information about the behavior of certain nano-based therapeutics once they are aerosolized for pulmonary delivery, including their

¹Institute for Work and Health, University of Lausanne and Geneva, 1066 Epalinges-Lausanne, Switzerland.

²Ecole Polytechnique Fédérale de Lausanne, CH-1015 Lausanne, Switzerland.

³SAFENANO, IOM Singapore, 048622 Singapore.

agglomeration potential, deposited dose in the lung after inhalation, and subsequent fate in the human body. It is generally accepted that aerosol particles of 1–5 μm are required for deposition in the alveolar region of the lung, where there is the highest systemic absorption. The primary factors influencing the aerosol particle size and the site of the aerosol deposition include the design of the inhalation device and the physicochemical properties of the drug formulation.⁽⁵⁾ However, the lack of characterization information for nebulized nanotherapeutics marks an important research need in current nanomedicine efforts.

In this study, our interest was directed toward superparamagnetic iron oxide nanoparticles (SPIONs), which are synthetic $\gamma\text{-Fe}_2\text{O}_3$ (maghemite), Fe_3O_4 (magnetite), or $\alpha\text{-Fe}_2\text{O}_3$ (hermatite) particles with a core ranging from 10 nm to 100 nm in diameter.⁽⁶⁾ In the last decade, biomedical interest for SPIONs has increased significantly due to a number of useful properties, such as biocompatibility, biodegradability, and superparamagnetism. Specifically, SPIONs offer a promising application for targeted imaging and treatment of lung cancer.^(7,8) In particular, a growing community of researchers has been investigating the potential for targeted aerosol delivery to specific lung regions using SPIONs in combination with target-directed magnetic gradient fields.^(9,10) SPIONs can also serve as theranostic agents, *i.e.*, as both diagnostic and therapeutic agents, where their inherent magnetic properties can provide image contrast in magnetic resonance imaging and thermal ablation in magnetic fluid hyperthermia therapy.⁽¹¹⁾ Moreover, as SPIONs can be chemically modified or engineered for simultaneous biomedical functions, their application as aerosolized chemotherapeutics may be used to increase drug dosage to the lungs while reducing systemic side effects.⁽¹²⁾

Numerous preclinical and clinical studies have been conducted using SPIONs, resulting in their clinical approval for intravenous (IV) and oral administration.^(13–16) However, SPIONs have yet to be administered as pulmonary therapeutic agents for treatment and prevention of lung disease. A recent review article summarizing both human and animal *in vivo* inhalation data on iron oxide particles suggests that controlled human exposure to iron oxide nanoparticles, such as SPIONs, could be conducted safely, and as such, marks SPIONs as strong candidates for application as aerosol-mediated nanotherapeutics.⁽¹⁷⁾ Nevertheless, it should duly be noted that despite clinical approval of selected SPION formulations for IV and oral administration, certain animal studies have questioned the biocompatibility of SPIONs and their lack of cytotoxicity following inhalation, specifically noting potential toxic effects due to macrophage clearance function overloading.⁽¹⁸⁾ To the authors' knowledge, no controlled human inhalation studies have been carried out with aerosolized SPIONs, and as such, increased research is necessary to ascertain the biocompatibility of these nanoparticles before their application for human pulmonary use.

Ferumoxytol [marketed under the names Feraheme (United States)/Rienso (European Union); referred to as Rienso throughout this article] is an industrially synthesized SPION formulation used for the IV treatment of iron deficiency anemia. As the only metal-based engineered nanoparticle approved by the US Food and Drug Administration and European Medicines Agency, it serves as a preferred candidate for controlled human exposure studies.⁽¹⁹⁾ Ferumox-

tytol is coated with a polyglucose sorbitol carboxymethyl ether (PSC), which is designed to minimize immunological sensitivity and to isolate the bioactive iron from plasma components until the nanoparticle enters macrophages in the reticuloendothelial system of the liver, spleen, and bone marrow. The iron is then released intracellularly within vesicles in macrophages where it can bind to ferritin or incorporate into hemoglobin.⁽²⁰⁾ Although the physical, pharmacokinetic, and biologic properties of ferumoxytol in therapeutic trials have been reported for IV injection,⁽²¹⁾ the authors are not aware of physicochemical characterization conducted on nebulized Rienso.

Materials and Methods

Nanoparticles

Rienso (lot 32327; Takeda Pharmaceuticals, Osaka, Japan) was purchased commercially from the University Hospital of Lausanne Pharmacy (Lausanne, Switzerland) in 17-mL glass vials. The manufacturer description presents Rienso as an aqueous colloidal solution consisting of non-stoichiometric magnetite (superparamagnetic iron oxide) coated with PSC, with elemental iron concentration of 30 mg/mL, mannitol at concentration of 44 mg/mL, water, and sodium hydroxide and hydrochloric acid for pH adjustments. The particle size was reported to be 17–30 nm, and the molecular weight given was 731 kDa. Upon receipt of the original vial, 1-mL aliquots were prepared in sterilized glass crimp vials under sterile conditions. The sterile aliquots were stored at the recommended temperature of 20°C before use, and diluted for the nebulization experiments before the marked expiration date.

Particle suspensions

Four concentrations of Rienso suspensions were prepared for nebulization by diluting 167 μL , 333 μL , 667 μL , and 1,333 μL of Rienso with 100 mL of GenPure water at room temperature to achieve suspension mass concentrations of 0.05 mg/mL, 0.1 mg/mL, 0.2 mg/mL, and 0.4 mg/mL, respectively. Rienso solutions were nebulized immediately after preparation over a 40-min period. Nebulization for each concentration was repeated three times. The suspension was characterized before and after the nebulization. Four complementary concentrations of mannitol (Rienso's primary excipient) were prepared to achieve mass concentrations of 0.07 mg/mL, 0.15 mg/mL, 0.29 mg/mL, and 0.59 mg/mL. As Rienso contains 44 mg/mL mannitol to 30 mg/mL Fe, it was deemed important to conduct separate mannitol nebulizations to deduce potential interactions between aerosolized SPIONs and mannitol particles.

Nebulization system

A custom nebulization system was used and consisted of a one-jet Collison nebulizer (BGI Incorporated, Waltham, MA, USA), glass mixing tube (length of 53.5 cm and diameter of 8.3 cm), and collection and measurement station. In this system (Fig. 1), the Collison nebulizer was fed by a 50-L cylinder of respirable air. A second airflow, technical air treated by a HEPA filter, led to the glass mixing tube in order to homogenize the two airflows and establish a stable humidity level. The dry air was also used to dry the aerosol,

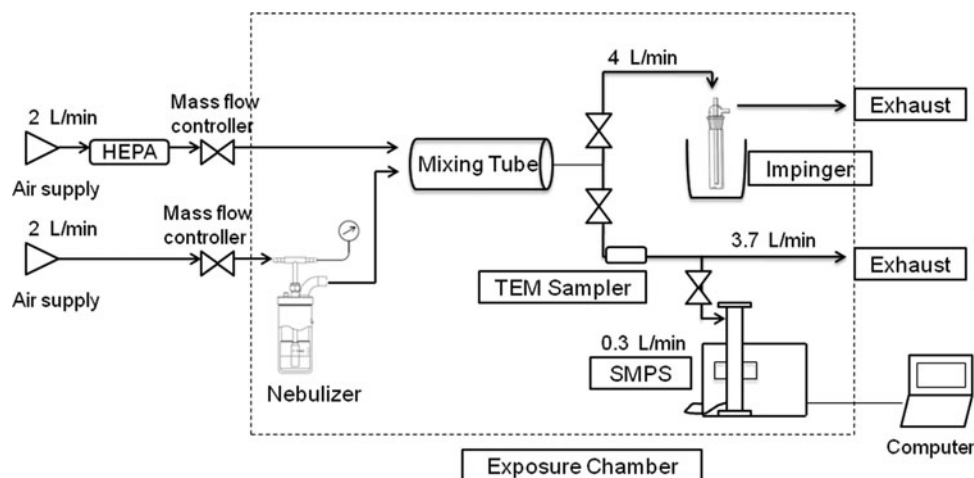


FIG. 1. Setup of the nebulization system.

which allowed for nano-sized particles versus micrometer-sized droplets to be measured. The aerosol was then directed to a collection and characterization station comprised of a scanning mobility particle sizer [SMPS; Grimm, Ainring, Germany; models 55-40-25 (CPC) and 5.403 (DMA)] to characterize the particle size distribution/number concentration of the aerosol, as well as an impinger to collect the aerosolized particles.

The nebulizer was operated at 20 pounds per square inch (psi) with a flow rate of 2 L/min from the air cylinder. The Collison nebulizer generates an aerosol by aspirating the suspension through a sonic-velocity jet, thus shearing the liquid into droplets. The Collison nebulizer was selected for this study as this specific nebulizer represents a validated instrument in aerosol research, known for its reliable generation of constant aerosol concentrations over extended periods of time with little change in particle size distribution.^(22,23) According to the manufacturer, droplets produced have a mass median diameter of 2 μm at 20 psi, and the liquid use rate of the nebulizer was 1.5 mL/hr. The second airflow to the mixing tube was set at a complementary rate of 2 L/min in order to obtain an average humidity of 50% throughout the exposure system. The mixing tube was then connected directly to the SMPS [Grimm Ainring; models 55-40-25 (CPC) and 5.403 (DMA)] for the characterization of particle size distribution/number concentration of the aerosol or to the impinger (filled with 20 mL of GenPure water and kept in ice).

Conductive tubing (Milian SA, Geneva, Switzerland) with an internal diameter of 8 mm was used with the shortest lengths possible to enhance particle transport and reduce particle loss to the tubing. A digital thermal mass flow meter and controller (Bronkhorst High-Tech BV, E Flow, Ruurlo, Netherlands) and a battery-powered thermal mass flow meter for gases (red-y compact meter; Vögtlin Instruments AG, Aesch, Switzerland) were added along the tubes of each airflow to ensure constant airflow.

Physicochemical characterization of Rienso

Particle concentration measurement methods. *Atomic absorption spectroscopy (AAS).* AAS measurements were carried out with a VARIAN AA240Z Zeeman (Varian, Inc., Palo Alto, CA, USA). Sterile Rienso was acid-digested us-

ing HNO_3 . The iron content was determined by redox titration, as well as by photometric measurements.

Magnetic susceptibility measurements (MSM). MSM were performed with an MS2G small sample sensor (Bartington Instruments Ltd., Witney, UK). Plotting the magnetic susceptibility as a function of the nanoparticle concentration shows a linear relationship. Magnetic susceptibility represents the degree of magnetization of materials in response to an applied magnetic field. For samples with constant volume, magnetic susceptibility increases with the magnetic nanoparticle concentrations, and MSM has shown to be a robust and quick method for detecting SPION concentration in suspensions.⁽²⁴⁾ However, it should duly be noted that at low concentrations, magnetic susceptibility is also dependent on the particle aggregation in suspension, and as such, MSM should be interpreted carefully, and in combination with complimentary methods, to predict SPION concentration.⁽²⁵⁾

Inductively coupled plasma optical emission spectroscopy (ICP-OES) and inductively coupled plasma mass spectrometry (ICP-MS). Spectrometry measurements were performed with an ICPE-9000 Multitype ICP Emission Spectrometer (Shimadzu, Kyoto, Japan) and an ELAN DRC II ICP mass spectrometer (PerkinElmer, Waltham, MA, USA). First, 100 μL of the sample was dissolved with 100 μL of hydrochloric acid (6 M) and then diluted 26 times with deionized and filtered water. ICP-OES was used for higher concentrations (0.05–0.4 mg/mL), and ICP-MS was preferred for the small concentrations of iron obtained in the impinger.

Scanning mobility particle sampler (SMPS). Aerodynamic diameter measurements were performed with an SMPS [Grimm; models 55-40-25 (CPC) and 5.403 (DMA)]. An average of three measurements was calculated.

Particle size measurement methods. *Photon correlation spectroscopy (PCS) measurements.* Light scattering measurements were carried out at 90° on a PCS (Brookhaven Instruments Corporation, Holtsville, NY, USA) equipped with a BI-90000AT digital autocorrelator. The CONTIN

method was used for data processing. The theoretical refractive index of 2.42 of magnetite⁽²⁶⁾ was used to calculate the number and volume-weighted distribution from the raw intensity data. Viscosity, refractive index, and the dielectric constant of pure water were used to characterize the solvent. Three measurements were taken for each sample and averaged.

Nanoparticle tracking analysis (NTA) measurements. NTA measurements were performed with a Nanosight LM series (Nanosight Ltd., Wiltshire, UK). All suspensions were diluted 100 times with GenPure water (except for impinger-collected suspensions). For all NTA assessments, an average of three measurements was calculated.

Transmission electron microscopy (TEM). A Phillips CM-20 microscope operating at 200 kV and Phillips CM-300 at 300 kV were used for high-resolution TEM. To assess the Rienso particles in solution, carbon-coated copper TEM grids were prepared by diluting Rienso 100 times in double-distilled, deionized water. This solution was then pipetted onto TEM grids and allowed to dry slowly overnight. To assess the Rienso particles in aerosol, carbon-coated copper TEM grids were secured in a Mini Particle Sampler (INERIS, Verneuil-en-Halatte, France) and attached within the nebulization system. A Rienso suspension at 0.1 mg/mL was prepared with GenPure water and nebulized in the system for 30 min at 6 L/min. The physical particle size distribution for Rienso particles both in suspension and in aerosol was estimated by measuring 100 particles at various magnifications. Image processing of TEM micrographs was performed with the software, ImageJ (National Institutes of Health, Bethesda, MD, USA).

Additional characterization measurement. Zeta potential. The zeta potential of the suspension was obtained with a ZetaPals analyzer (Brookhaven Instruments Corporation). Samples were diluted to 0.1 mg/mL with GenPure water, and an average of three measurements was calculated.

Bacterial sterility. Rienso stock solution was aliquoted in sterile glass containers and smeared on Tryptic Soy Agar plates (Sigma-Aldrich, St. Louis, MO, USA) once every 3 days for a total of four consecutive weeks. The smeared plates were incubated at 25°C. One blank and one positive control (Rienso + mouth swab) were prepared on the first day of sterility testing. As the Rienso SPION is coated with PSC, a carbohydrate, and several aliquots were obtained from each sterile Rienso container, it was deemed necessary to determine if the aliquoting technique introduced contamination into the sample.

Results and Discussion

Characterization of Rienso stock solution

Prior to the nebulization experiments, the stock solution (Rienso, Takeda Pharmaceuticals, lot 32327) was characterized to confirm the manufacturer description. PCS was used to test the stability of the nanoparticles in water, phosphate-buffered saline, and Dulbecco's modified Eagle medium at 37°C. Over 44 hr, the mean hydrodynamic diameter was 22 ± 2 nm, 22 ± 2 nm, and 23 ± 3 nm in all three

solutions, demonstrating the stability of the original nanoparticle size in the various media. The stability of the particle size in suspension over time in various media denotes an important feature for future studies due to the ability to ensure standardized exposure parameters. To confirm Rienso concentration (manufacturer description: 30 mg/mL Fe), AAS measurements were carried out, and an iron concentration of 29.9 mg/mL Fe was determined. In order to evaluate compatibility of Rienso as a test substance for potential application in therapeutic aerosol studies, and to determine if aliquoting introduced contamination into the sample, the sterility of the solution was assessed. Bacterial growth was confirmed to be negative for Rienso aliquots for up to 4 weeks. Only the positive control (Rienso + mouth swab) yielded bacteria colonies from day 1.

For the nebulization experiments, we will first describe the results of the characterized nanoparticles in the initial suspension before nebulization. These results will be compared with the suspension in the nebulizer after undergoing 40 min of nebulization, and the suspension re-collected in the impinger after nebulization. The characterization of the aerosolized particles will then be discussed.

Characterization of Rienso in suspension

Analysis of TEM micrographs of Rienso suspension revealed the mean diameter number (d_n)⁽²⁷⁾ to be 9 ± 2 nm (Fig. 2). The TEM micrographs further demonstrate that the electron dense particles are approximately uniform in size.

The four Rienso suspensions (0.05 mg/mL, 0.1 mg/mL, 0.2 mg/mL, and 0.4 mg/mL) were characterized prior to nebulization (see Table 1). NTA demonstrated an average number weighted hydrodynamic diameter of 60 ± 8 nm, 56 ± 1 nm, 48 ± 4 nm, and 60 ± 4 nm, respectively.

Light scattering measurements conducted with PCS demonstrated a number weighted average diameter (d_n) of 13 ± 5 nm, 27 ± 7 nm, 24 ± 3 nm, and 21 ± 5 nm, respectively.

After nebulization, the size of the nanoparticles remained similar to those of the initial four suspensions with NTA measurements of 64 ± 1 nm, 52 ± 2 nm, 72 ± 7 nm, and 67 ± 3 nm, respectively. PCS measurements of the suspension after nebulization also demonstrated an overall stability of particle

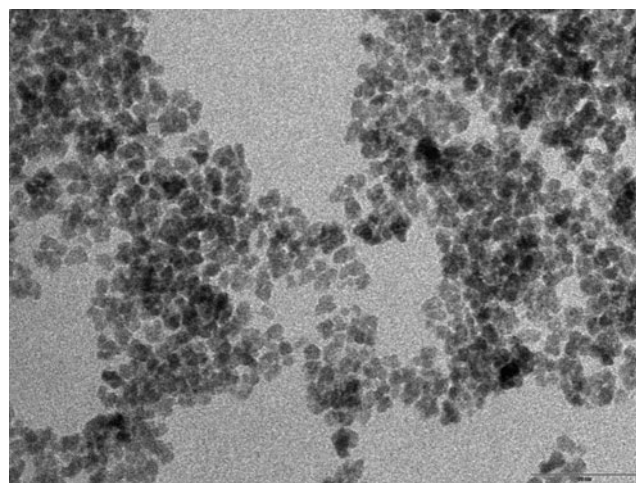


FIG. 2. High-resolution TEM micrograph showing Rienso in the 10-nm range (scale bar = 50 nm).

TABLE 1. PROPERTIES OF RIENSO SUSPENSIONS AS MEASURED BY PCS, NTA, AND ZETA POTENTIAL BEFORE NEBULIZATION, AFTER NEBULIZATION, AND AFTER COLLECTION BY IMPINGER

Sample	Concentration (mg/mL)	PCS average number weighted size (nm)	NTA average number weighted size (nm)	Zeta potential (mV)
Before nebulization	0.05	13 ± 5	60 ± 8	-38 ± 1
	0.1	27 ± 7	56 ± 1	-40 ± 3
	0.2	24 ± 3	48 ± 4	-42 ± 1
	0.4	21 ± 5	60 ± 4	-40 ± 1
After nebulization	0.05	17 ± 1	64 ± 1	-44 ± 1
	0.1	23 ± 2	52 ± 2	-43 ± 3
	0.2	23 ± 5	72 ± 7	-46 ± 2
	0.4	24 ± 10	67 ± 3	-42 ± 1
Impinger	0.05	—	156 ± 56	—
	0.1	—	159 ± 46	—
	0.2	—	124 ± 19	—
	0.4	—	103 ± 5	—

diameter (d_n) with 17 ± 1 nm, 23 ± 2 nm, 23 ± 5 nm, and 24 ± 10 nm, respectively, for each concentration.

Following nebulization, the aerosol was re-collected in the impinger and the particle sizes were measured with NTA, but not with PCS, as the concentration was in the $\mu\text{g}/\text{mL}$ range and therefore too low to be measured with the latter. The impinger results demonstrated that the particle size increased considerably to 156 ± 56 nm, 159 ± 46 nm, 124 ± 19 nm, and 103 ± 5 nm for each of the concentrations, respectively. These results suggest that the size of the particles did not vary in the nebulizer before and after nebulization, but increased considerably due to the most likely formation of agglomerates during resolubilization from an aerosol to a liquid. The results further demonstrate that the initial concentration does not influence the hydrodynamic diameter of the particles measured in the impinger.

It is important to note that the size discrepancy between the particle size measured with TEM, PCS, and NTA results from the fact that whereas TEM examines individual core nanoparticles, PCS is an ensemble measurement that measures effective diameter based on light scattering. NTA, on the other hand, measures the effective diameter based on particles' Brownian motion. In other words, TEM provides a mean diameter number measurement of primary particles, whereas PCS and NTA provide a hydrodynamic diameter measurement of primary aggregates.⁽¹⁸⁾

The zeta potential of the Rienso nanoparticles was measured before and after nebulization at each concentration and demonstrated an insignificant change overall. Rienso nanoparticles in the initial solution demonstrated -38 ± 6 mV, -40 ± 3 mV, -42 ± 1 mV, and -40 ± 1 mV at 0.05 mg/mL, 0.1 mg/mL, 0.2 mg/mL, and 0.4 mg/mL, respectively. In the solutions after nebulization, Rienso nanoparticles demonstrated -44 ± 1 mV, -43 ± 3 mV, -46 ± 2 mV, and -42 ± 1 mV at 0.05 mg/mL, 0.1 mg/mL, 0.2 mg/mL, and 0.4 mg/mL, respectively. The zeta potentials of the Rienso nanoparticles before and after nebulization demonstrate a minimal increase after collection in the impinger. We were unable to measure the charge distribution of the suspension obtained in the impinger due to the extremely low concentration of Rienso nanoparticles ($\mu\text{g}/\text{mL}$ range). From these results, we may conclude that no trend was observed and that the zeta potential remained constant between the initial solution and the nebulized solution. It has been reported that

negatively charged particles are retained in the lungs more efficiently than positively charged particles; therefore, the negative charge of the Rienso particles throughout the nebulization process gives a potential advantage for this SPION formulation if applied therapeutically.⁽²⁸⁾

Concentration of iron in Rienso suspension following nebulization

The concentration of SPIONs was obtained from magnetic susceptibility measurements and from ICP-OES for the suspension before and after nebulization and from ICP-MS for the suspension in the impinger (Fig. 3). Overall, we observed a slight increase in concentration in the nebulizer after nebulization, which is explained by a loss of approximately 3 mL of water during nebulization from the formation of droplets in the aerosol containing the Rienso particles. The concentration of SPIONs in the impinger was very small compared with the initial SPION concentration. Nevertheless, the same trend is observed; as the initial concentration increases, the concentration tends to increase in the impinger. When comparing the results of the two methods, a slight difference is observed, which may be due

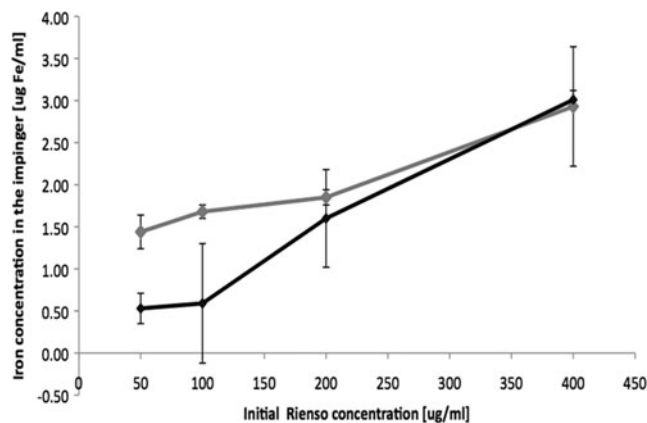


FIG. 3. Iron concentration in the impinger over the initial concentration measured with ICP-MS (gray) and magnetic susceptibility (black).

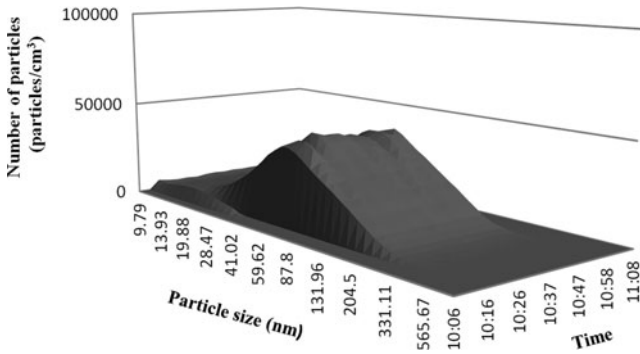


FIG. 4. Number of particles (particle concentration) and particle size over time at 0.05 mg/mL as measured by the SMPS.

to the fact that the concentration is at the limit of detection for the MS2G small sample sensor. It is likewise important to note that the standard error observed with the MS2G small sample sensor is larger due to the higher detection limit, which is 2×10^{-6} SI ($2 \mu\text{g}$ of Fe/mL) compared with the detection limit of the ICP-MS, of 1 ppt (1 ng of Fe/L). The difference between ICP-MS and MSM may also be due to particle aggregation occurring in suspension, thereby resulting in lower concentration values as measured by the MS2G small sample sensor. However, when interpreted together, these two complimentary methods confirm the presence of iron, and therefore of SPIONs, in the impinger due to the nebulization process.

Characterization of Rienso suspension in the aerosol

The total number of aerosolized particles and their aerodynamic diameter over the 40-min nebulization were measured with the SMPS. For each of the four concentrations, a peak concentration at a reproducible particle size of about 70 nm was observed. The intensity of this peak increased as the initial concentration increased from approximately 45,000 particles/cm³ at 0.05 mg/mL to approximately 80,000 particles/cm³ at 0.4 mg/mL (Figs. 4 and 5). This result demonstrates that the number of SPIONs in each droplet most likely increased as the initial concentration in-

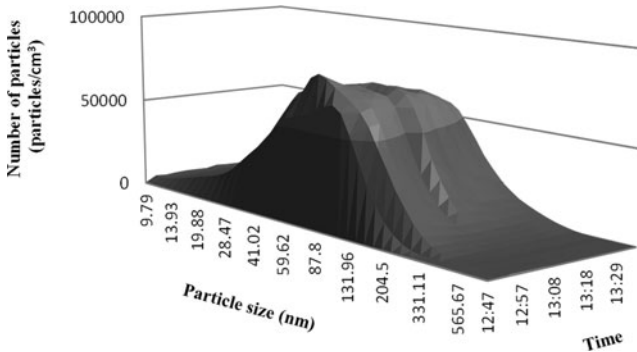


FIG. 5. Number of particles (particle concentration) and particle size over particle size at 0.4 mg/mL as measured by the SMPS.

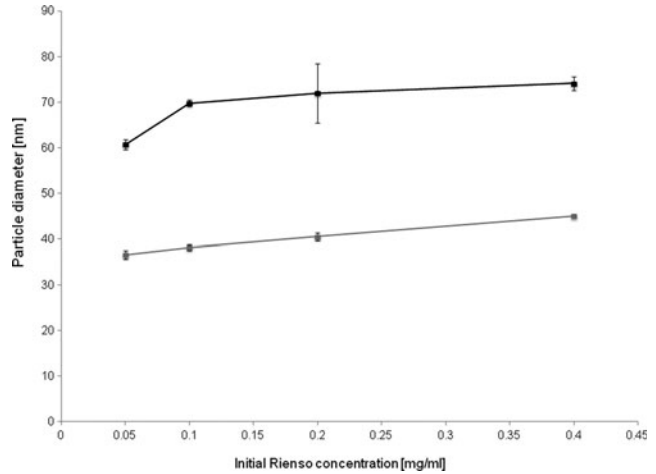


FIG. 6. Size of the particles in the aerosol measured with the SMPS at 0.05 mg/mL, 0.1 mg/mL, 0.2 mg/mL, and 0.4 mg/mL concentrations of Rienso (black) and mannitol (gray).

creased, resulting in an overall increase in the concentration of SPIONs in the aerosol.

In addition to this, it is important to note that the total number of aerosolized particles and their aerodynamic diameter are reproducible for each concentration. This represents an important feature for future applications, as these results demonstrate that the particle size and number distribution are directly correlated to the initial concentration of the Rienso suspension. The size of the particles in the aerosol tends to increase slightly as the initial concentration increases, which is most likely due to increased particle agglomeration in the aerosol due to a larger concentration of aerosolized particles overall (Fig. 6). With a greater concentration of particles in the aerosol, the propensity for particle-to-particle attraction and agglomeration is increased when compared with lower concentrations. In this series of

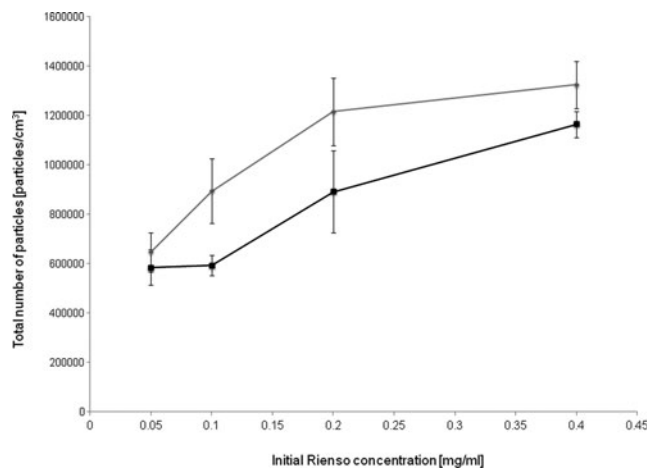


FIG. 7. Total number of particles measured in the aerosol with the SMPS at 0.05 mg/mL, 0.1 mg/mL, 0.2 mg/mL, and 0.4 mg/mL concentrations of Rienso (black) and mannitol (gray).

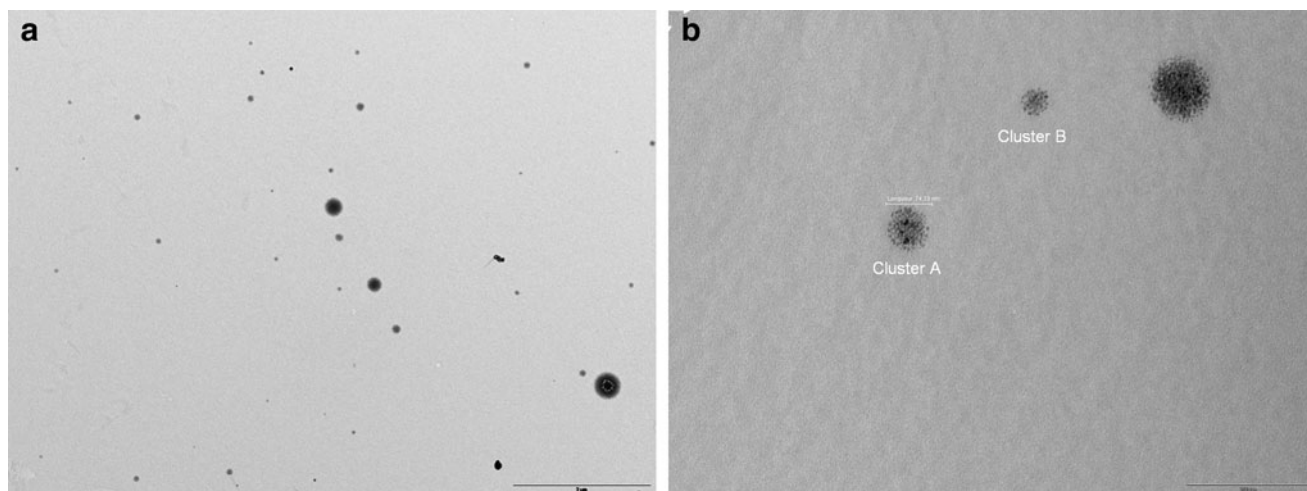


FIG. 8. High-resolution TEM micrograph of aerosolized Rienso collected on a TEM grid. (a) Scale bar = 2 μm. (b) Scale bar = 200 nm.

nebulizations, the particle size distribution demonstrates a plateau at approximately 75 nm.

The general trend observed with the total number of particles over time is a sharp increase over the first 10 min up to a plateau point. This plateau point tends to increase as the initial concentration is increased due to a greater number of particles in the nebulized droplets. The total number of particles measured for each Rienso suspension concentration is plotted in Figure 7. The total number of particles in the aerosol is doubled from 0.1 mg/mL with around 600,000 particles/cm³ to 0.4 mg/mL with around 1,200,000 particles/cm³.

As previously noted, the interaction of nanoparticles with lung cells depends on the size of the particles.⁽²⁹⁾ An in-

crease in the size of the particle due to agglomeration may promote their clearance via macrophages and could greatly influence the location of drug release. This indicates that changes in the size of the aerosolized nanoparticles may affect the drug dose and release kinetics. Nevertheless, the particle agglomeration in this study remained below 100 nm, which suggests an effective deposition in the alveolar region of the lung.

The primary excipient of Rienso, mannitol, was also nebulized at four complementary concentrations to the Rienso solutions in order to characterize its aerodynamic diameter and concentration in aerosol form. The series of mannitol nebulizations, when compared with the Rienso nebulizations, reveals two important observations. First, the total

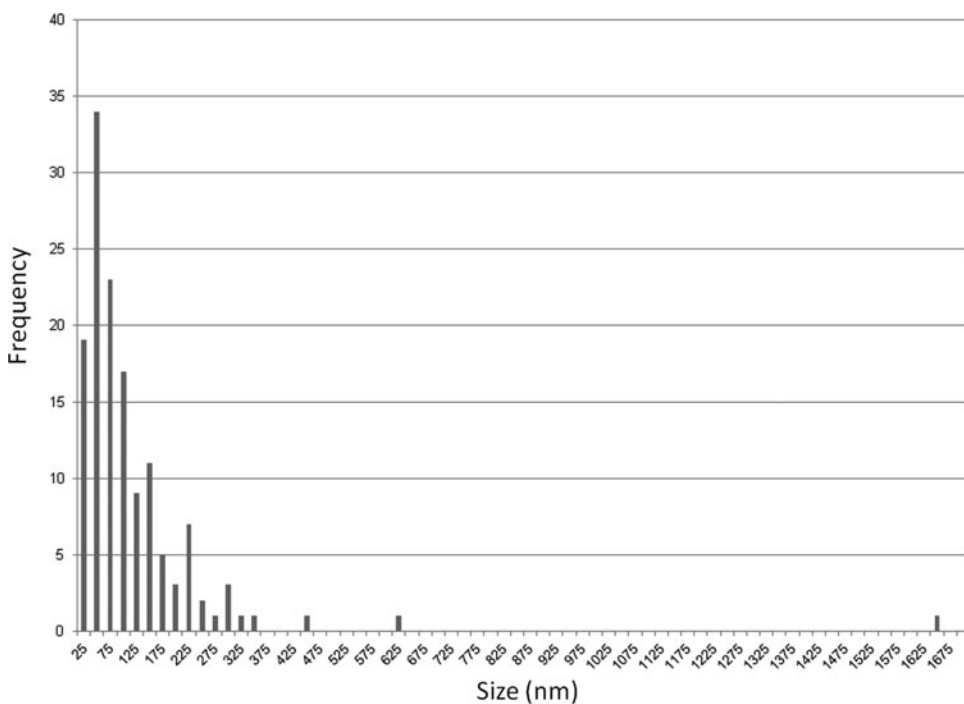


FIG. 9. Histogram of ImageJ analysis of Figure 8 demonstrating frequency distribution of size of agglomerated Rienso particles following nebulization.

concentration of aerosolized particles was similar to that of the Rienso formulation (Fig. 7), albeit slightly higher. Secondly, the aerodynamic diameter of the particles was smaller, in the range of 35–45 nm (Fig. 6) compared with Rienso in the range of 60–70 nm. Several studies have highlighted the advantages of using mannitol in aerosolized therapeutics formulations.^(30,31) The desirability of using nebulized mannitol is largely a result of its minimal airway transepithelial permeability, resulting in a longer duration of therapeutic action, as well as its pleasant taste and mouth feel for encouraging patient use.^(32,33)

Aerosolized Rienso particles were also captured on a TEM grid and analyzed to compare with the Rienso particles in the suspension. Image analysis of aerosolized Rienso particles by TEM demonstrated an overall pattern of monodispersed spherical particles, comprised of agglomerates of primary particles (Fig. 8). In Figure 8b, a total of 32 primary particles that comprise Cluster A were analyzed and were determined to have an average diameter of 9 ± 2 nm. A total of 20 primary particles that comprise Cluster B were also analyzed and were determined to have an average diameter of 8 ± 1 nm (Fig. 8b). A full image analysis (ImageJ, USA) of agglomerated particles in Figure 8 demonstrated a mean diameter of approximately 75 nm of each cluster (Fig. 9).

The ultimate aim of this study was to characterize Rienso SPIONs before and after nebulization to deduce the effects of aerosolization on particle properties. Although it was hypothesized that the change of state from suspension to aerosol would induce effects on the physical particle size, the question remained: how would the particles undergo alterations in this process specifically, and what would be their agglomeration behavior? By assessing the initial Rienso suspension, we demonstrated a primary particle mean diameter of approximately 9 ± 2 nm, as measured by TEM analysis, which provides a value of the electron dense iron core. When measured by PCS, a measurement that takes into account hydrodynamic diameter of the colloidal particle, we observed a particle size that correlated with the manufacturer's description of 17–30 nm with an average hydrodynamic particle diameter of 25 ± 3 nm. Analysis of nebulized Rienso particles demonstrates clustering of primary particles and the formation of agglomerates that are in the approximate size range of the values collected by the SMPS. The formation of Rienso agglomerates in the aerosol can be explained by the inherent principles of nebulization. As the Rienso suspension is aspirated through the sonic-velocity jet, the liquid is sheared into droplets approximately $2 \mu\text{m}$ in size. Upon meeting the air, these droplets dry and evaporate, inducing the agglomeration of primary particles into larger clusters. This assertion is supported by the TEM micrographs before and after nebulization, the former demonstrating primary particle size of 9 nm, and the latter demonstrating 9 nm primary particles agglomerated into clusters approximately 75 nm in diameter. This observation directly correlates with aerosol data from the SMPS, which demonstrated an average aerodynamic particle diameter of approximately 70–75 nm.

As the aerosol was recondensed in the impinger, we observed a significant increase in particle diameter. As particle agglomerates in the aerosol are rehydrated in the impinger, it is possible that they are undergoing further agglomeration

with proximal particles to form larger clusters. This assertion is supported by NTA data, which overall demonstrate a larger hydrodynamic particle diameter for particles recondensed in the impinger after undergoing nebulization compared with the particles before nebulization. This observation is critical for clinical therapeutic aerosol research, as aerosolized particles that meet the air–liquid interface of the lungs will be resolubilized. Thus, understanding the kinetics of particle agglomeration and resulting particle size proves imperative for accurate estimation of targeted lung dose of aerosolized nanoparticles. Further research on aerosolized SPION characterization is needed to further elucidate these preliminary observations.

Conclusion

In this article, we have used various characterization techniques to deduce the effects of nebulization on the physical particle size and concentration of Rienso, a commercially available ferumoxytol SPION formulation. Overall, it was determined that the size of the nanoparticles in suspension did not change after nebulization, but did form agglomerates in the aerosol. The size and concentration of the particles in the aerosol tended to increase as the initial suspension concentration increased. The concentration of iron in the impinger after nebulization followed the same trend, with the SPION concentration in the impinger increasing as the initial concentration increased. To the authors' knowledge, this study marks the first independent characterization of aerosolized Rienso and, as such, provides critical information on the behavior of Rienso nanoparticles in an aerosol. The data obtained in this study add new knowledge for the existing body of literature on potential applications of ferumoxytol suspensions as inhaled aerosol therapeutics.

Acknowledgments

The authors would like to thank the Swiss National Science Foundation, NRP 64 Project, Grant No. 406440_131282 for funding doctoral research of H.G. and the Whitaker International Program for funding the postdoctoral grant to N.L. The authors also thank Antonio Mucciolo, University of Lausanne, Switzerland, for assistance in TEM grid preparation and TEM sample analysis.

Author Disclosure Statement

The authors declare that there are no conflicts of interest.

References

1. O'Hagan DT, and Illum L: Absorption of peptides and proteins from the respiratory tract and the potential for development of locally administered vaccine. *Crit Rev Ther Drug Carrier Syst.* 1990;7:35–97.
2. Geiser M, and Kreyling W: Deposition and biokinetics of inhaled nanoparticles. *Part Fibre Toxicol.* 2010;7:2.
3. Kreyling WG, Möller W, Semmler-Behnke M, and Oberdörster G: Particle dosimetry: deposition and clearance from the respiratory tract and translocation towards extrapulmonary sites. In: K Donaldson, and P Borm, (eds). *Particle Toxicology.* CRC Press, Taylor & Francis Group, Boca Raton, FL; pp. 47–74, 2007.

4. Bailey MM, and Berklund CJ: Nanoparticle formulations in pulmonary drug delivery. *Med Res Rev.* 2009;29:196–212.
5. McCallion ON, Taylor KM, Thomas M, and Taylor AJ: Nebulization of fluids of different physicochemical properties with air-jet and ultrasonic nebulizers. *Pharm Res.* 1995;12:149–164.
6. Wahajuddin, and Arora S: Superparamagnetic iron oxide nanoparticles: magnetic nanoplatforms as drug carriers. *Int J Nanomed.* 2012;7:3445–3471.
7. Yoo MK, Park IK, Lim HT, Lee SJ, Jiang HL, Kim YK, Choi YJ, Cho MH, and Cho CS: Folate-PEG-superparamagnetic iron oxide nanoparticles for lung cancer imaging. *Acta Biomater.* 2012;8:3005–3013.
8. Parcell KL, Kalber TL, Walker-Samuel S, Southern P, Pankhurst QA, Lythgoe MF, and Janes SM: S89 Bimodal iron oxide nanoparticles for hyperthermia therapy and MR imaging in cancer. *Thorax.* 2010;65(Suppl 4):A41–A42.
9. Upadhyay D, Scalia S, Vogel R, Wheate N, Salama RO, Young PM, Traini D, and Chrzanowski W: Magnetised thermo responsive lipid vehicles for targeted and controlled lung drug delivery. *Pharm Res.* 2012;29:2456–2467.
10. Tewes F, Ehrhardt C, and Healy AM: Superparamagnetic iron oxide nanoparticles (SPIONs)-loaded Trojan micro-particles for targeted aerosol delivery to the lung. *Eur J Pharm Biopharm.* 2014;86:98–104.
11. Hofmann-Amtentbrink M, von Rechenberg B, and Hofmann H: Superparamagnetic nanoparticles for biomedical applications. In: MC Tan, G Chow, and L Ren, (eds). *Nanos-structured Materials for Biomedical Applications*. Transworld Research Network, Kearala, India; pp. 119–149, 2009.
12. Verma NK, Crosbie-Staunton K, Satti A, Gallagher S, Ryan KB, Doody T, McAtamney C, MacLoughlin R, Galvin P, Burke CS, Volkov Y, and Gun'ko YK: Magnetic core-shell nanoparticles for drug delivery by nebulization. *J Nanobiotechnol.* 2012;11:1.
13. Bernd H, De Kerviler E, Gaillard S, and Bonnemain B: Safety and tolerability of ultrasmall superparamagnetic iron oxide contrast agent: comprehensive analysis of a clinical development program. *Invest Radiol.* 2009;44:336–342.
14. Bourrinet P, Bengel H, Bonnemain B, Dencausse A, Idee JM, Jacobs PM, Lewis JM: Preclinical safety and pharmacokinetic profile of ferumoxtran-10, an ultrasmall superparamagnetic iron oxide magnetic resonance contrast agent. *Invest Radiol.* 2006;41(3):313–324.
15. Corot C, Robert P, Idee JM, and Port M: Recent advances in iron oxide nanocrystal technology for medical imaging. *Adv Drug Deliv Rev.* 2006;58:1471–1504.
16. Hahn P, Stark DD, Lewis JM, Saini S, Elizondo G, Weissleder R, Fretz CJ, and Ferrucci JT: First clinical trial of a new superparamagnetic iron oxide for use as an oral gastrointestinal contrast agent in MR imaging. *Radiology.* 1990;175:695–700.
17. Lewinski N, Graczyk H, and Riediker M: Human inhalation exposure to iron oxide particles. *BioNanoMaterials.* 2013; 14(1–2):5–23.
18. Zhu MT, Feng WY, Wang Y, Wang B, Wang M, Ouyang H, Zhao YL, and Chai ZF: Particokinetics and extrapulmonary translocation of intratracheally instilled ferric oxide nanoparticles in rats and the potential health risk assessment. *Toxicol Sci.* 2009;107:342–351.
19. Lu M, Cohen MH, Rieves D, and Pazdur R: FDA report: Ferumoxytol for intravenous iron therapy in adult patients with chronic kidney disease. *Am J Hematol.* 2010;85: 315–319.
20. Pai AB, and Garba AO: Ferumoxytol: a silver lining in the treatment of chronic kidney disease or another dark cloud. *J Blood Med.* 2012;3:77–85.
21. Landry R, Jacobs PM, Davis R, Shenouda M, and Bolton WK: Pharmacokinetic study of ferumoxytol: a new iron replacement therapy in normal subjects and hemodialysis patients. *Am J Nephrol.* 2005;25:400–410.
22. May KR: The Collison Nebulizer. Description, performance and application. *J Aerosol Sci.* 1973;4:235.
23. Gussman RA: Note on the particle size output of collision nebulizers. *Am Ind Hyg Assoc J.* 1984;45:B8–B12.
24. Maurizi L, Sakulku U, Gramoun A, Vallee JP, and Hofmann H: A fast and reproducible method to quantify magnetic nanoparticle biodistribution. *Analyst.* 2014;139:1184–1191.
25. Hong CY, Wu CC, Chiu YC, Yang SY, Horng HE, and Yang HC: Magnetic susceptibility reduction method for magnetically labeled immunoassay. *Appl Phys Lett.* 2006; 88:212512–212513.
26. Cornell RM, and Schwertmann U: *The Iron Oxides: Structures, Properties, Reactions, Occurrences and Uses*. VCH Verlagsgesellschaft GMBH, Weinheim, Germany; pp. 533–559, 1996.
27. Bowen P: Particle size distribution measurement from millimeters to nanometers and from rods to platelets. *J Dispers Sci Technol.* 2002;23:631–662.
28. Fidler IJ, Raz A, Fogler WE, Kirsh R, Bugelski P, and Poste G: Design of liposomes to improve delivery of macrophage-augmenting agents to alveolar macrophages. *Cancer Res.* 1980;40:4460–4466.
29. Griese M, and Reinhardt D: Smaller sized particles are preferentially taken up by alveolar type II pneumocytes. *J Drug Target.* 1998;5:471–479.
30. Chan JG, Traini D, Chan HK, Young PM, and Kwok PC: Delivery of high solubility polyols by vibrating mesh nebulizer to enhance mucociliary clearance. *J Aerosol Med Pulm Drug Deliv.* 2012;25:297–305.
31. Chan JG, Kwok PC, Young PM, Chan HK, and Traini D: Mannitol delivered by vibrating mesh nebulisation for enhancing mucociliary clearance. *J Pharm Sci.* 2011;100: 2693–2702.
32. Daviskas E, Anderson SD, Jaques A, and Charlton B: Inhaled mannitol improves the hydration and surface properties of sputum in patients with cystic fibrosis. *Chest.* 2010;137:861–868.
33. Minasian C, Wallis C, Metcalfe C, and Bush A: Comparison of inhaled mannitol, daily rhDNase and a combination of both in children with cystic fibrosis: a randomised trial. *Thorax.* 2010;65:51–56.

Received on December 10, 2013
in final form, March 6, 2014

Reviewed by:
Heidi Mansour
Frederic Tewes

Address correspondence to:
Dr. Michael Riediker
Institut de Santé au Travail
Rte de la Corniche 2
1066 Epalinges-Lausanne
Switzerland

E-mail: michael.riediker@alumni.ethz.ch